(2)

BASIC CONSIDERATION OF THE LIFTING CAPABILITY OF STOPPABLE ROTORS

by

Alan W. Schwartz

AVIATION AND SURFACE EFFECTS DEPARTMENT

DTNSRDC/ASED-84/10

December 1984

DAVID W. TAYLOR NAVAL SHIP RESEARCH AND DEVELOPMENT CENTER

BETHESDA
MARYLAND
20084

UNCLASSIFIED

SECURITY CLASSIFICATION OF THIS PAGE *(When Data Entered)*

REPORT DOCUMENTATION PAGE		READ INSTRUCTIONS BEFORE COMPLETING FORM
1. REPORT NUMBER DTNSRDC/ASED-84/10	2. GOVT ACCESSION NO. AD-A150850	3. RECIPIENT'S CATALOG NUMBER
4. TITLE *(and Subtitle)* BASIC CONSIDERATION OF THE LIFTING CAPABILITY OF STOPPABLE ROTORS		5. TYPE OF REPORT & PERIOD COVERED Final Report 6. PERFORMING ORG. REPORT NUMBER
7. AUTHOR(s) Alan W. Schwartz		8. CONTRACT OR GRANT NUMBER(s)
9. PERFORMING ORGANIZATION NAME AND ADDRESS David Taylor Naval Ship R&D Center Aviation and Surface Effects Department Bethesda, Maryland 20084		10. PROGRAM ELEMENT, PROJECT, TASK AREA & WORK UNIT NUMBERS ARPA Order 4238 Program Element 62711E Work Unit 1-1690-103
11. CONTROLLING OFFICE NAME AND ADDRESS Defense Advanced Research Projects Agency 1400 Wilson Boulevard Arlington, VA 22209		12. REPORT DATE December 1984 13. NUMBER OF PAGES 19
14. MONITORING AGENCY NAME & ADDRESS *(if different from Controlling Office)*		15. SECURITY CLASS. *(of this report)* UNCLASSIFIED 15a. DECLASSIFICATION/DOWNGRADING SCHEDULE

16. DISTRIBUTION STATEMENT *(of this Report)*

APPROVED FOR PUBLIC RELEASE: DISTRIBUTION UNLIMITED

17. DISTRIBUTION STATEMENT *(of the abstract entered in Block 20, if different from Report)*

18. SUPPLEMENTARY NOTES

19. KEY WORDS *(Continue on reverse side if necessary and identify by block number)*

Helicopters
Stoppable Rotors
Circulation Control

20. ABSTRACT *(Continue on reverse side if necessary and identify by block number)*

Stoppable rotor designs involve the operation of the rotor through very high advance ratios and, thus, large regions of reverse flow as the rotor is slowed. Dual-slot, circulation control airfoils, such as those on an X-Wing rotor, produce useable lift in the reverse flow region. A simple method is developed to determine the critical flight condition where the capability of the rotor to produce lift is minimized.

over

DD FORM 1 JAN 73 1473 EDITION OF 1 NOV 65 IS OBSOLETE
S/N 0102-LF-014-6601

UNCLASSIFIED

SECURITY CLASSIFICATION OF THIS PAGE *(When Data Entered)*

(cont

Expressions are derived relating the rotor retreating side mean dynamic pressure (indicative of lifting capability) and the lateral offset of the centroid of that dynamic pressure (indicative of roll moment capability) to the rotor geometry and flight conditions. The critical advance ratios predicted by these expressions are compared with the results from a more sophisticated rotor performance analysis. Keywords include: Helicopters, and Circulation control.

TABLE OF CONTENTS

LIST OF FIGURES

NOTATION

a	Unblown airfoil lift-curve slope, $dC_\ell/d\alpha$
C_ℓ	Sectional lift coefficient
C_μ	Momentum coefficient, $\dot{m}V_j/(q_\infty c)$
c	Chord length
$\dot{m}$	Mass efflux, slugs/sec
q	Dynamic pressure
R	Rotor radius
r	Blade spanwise location
V_j	Jet velocity
V_T	Tip rotational velocity
V_∞	Forward velocity
x	Dimensionless spanwise position, r/R
α	Sectional angle of attack
ε_{RS}	Lateral offset of qc centroid
λ	Blade taper ratio, C_{tip}/C_{root}
μ	Rotor advance ratio, $V_\infty/\Omega R$
ψ	Blade azimuth angle
Ω	Rotor rotational rate, $d\psi/dt$

ABSTRACT

Stoppable rotor designs involve the operation of the rotor through very high advance ratios and, thus, large regions of reverse flow as the rotor is slowed. Dual-slot, circulation control airfoils, such as those on an X-Wing rotor, produce useable lift in the reverse flow region. A simple method is developed to determine the critical flight condition where the capability of the rotor to produce lift is minimized. Expressions are derived relating the rotor retreating side mean dynamic pressure (indicative of lifting capability) and the lateral offset of the centroid of that dynamic pressure (indicative of roll moment capability) to the rotor geometry and flight conditions. The critical advance ratios predicted by these expressions are compared with the results from a more sophisticated rotor performance analysis.

ADMINISTRATIVE INFORMATION

The work presented was conducted at the David Taylor Naval Ship Research and Development Center (DTNSRDC) for the Defense Advanced Research Projects Agency under ARPA order 4238, DTNSRDC Work Unit 1-1690-103.

INTRODUCTION

Dual-slot, circulation control (CC) rotors, such as those used on an X-Wing aircraft, have an advantage over conventional rotors in that they produce useable lift within the reverse flow region. Therefore, these rotors are not limited by a maximum advance ratio at which the reverse flow region becomes so large as to preclude the rotor from producing the required lift. There is, however, a critical advance ratio, μ_{crit}, at which the rotor reaches a minimum lifting capability.

It is assumed that the mean dynamic pressure trends are indicative of relative rotor lifting capability. Thus, an analysis of the mean dynamic pressure on the retreating side of a rotor disk can be used to predict the critical operating condition.

Three typical conversion schedules for an X-Wing rotor are analyzed. These schedules are depicted in Figure 1. Schedules A and B represent rotor rpm reduction at constant forward speed, V_∞. Schedule C is a combined reduction of rotor rpm and increase in V_∞ such that $\Omega R + V_\infty$ is constant throughout the conversion. Comparison is made with the results for a conventional rotor having no reverse flow lifting capability. Also, application of the analysis to blade

planform design considerations is discussed. The results of this analysis are compared with those of a rigorous rotor performance prediction analysis.

DISCUSSION

Unlike conventional airfoils, the lift of CC airfoils is not a linear function of the dynamic pressure; therefore, the assumed relationship between mean dynamic pressure and rotor lifting capability deserves some attention. The empirical expression for lift coefficient

$$C_\ell = a \cdot \alpha + (dC_\ell/dC_\mu) \cdot C_\mu$$

is composed of terms representing the lift coefficient due to incidence and the lift coefficient due to blowing. The second term is of particular interest because it is nonlinear within the operating environment of the CC rotor blade element.

The blowing momentum coefficient

$$C_\mu = \dot{m}V_j/qc$$

is inversely proportional to the local dynamic pressure so that the local lift ($L = qcC_\ell$) is not directly affected by any dynamic pressure effect on C_μ. However, the blowing augmentation ratio, dC_ℓ/dC_μ, is known to be nonlinear, particularly at the higher C_μ levels where C_ℓ is linearly proportional to $\sqrt{C_\mu}$. This nonlinearity, combined with the effects of Mach number and slot height, causes lift due to blowing to be dependent (but not linearly dependent) upon q. For a typical X-Wing conversion condition, the C_ℓ equation is dominated by the blowing term. Hence, quantitative comparisons between relative rotor mean dynamic pressure and relative rotor lift may not be meaningful. Rather, the trends should be used to identify critical operating conditions which merit closer attention.

By integrating the local dynamic pressure over the blade span ($0 \leq r \leq R$) and over the retreating side of the rotor disk ($\pi \leq \psi \leq 2\pi$), an algebraic expression for the mean dynamic pressure can be derived as follows:

$$\bar{q} = \frac{\int_\pi^{2\pi} \int_0^R q(r,\psi)\, r\,dr\,d\psi}{\int_\pi^{2\pi} \int_0^R r\,dr\,d\psi} \qquad (1)$$

$$\bar{q} = \frac{2\rho}{\pi} V_T^2 \left(\frac{\pi}{8} - \frac{2}{3}\mu + \frac{\pi}{8}\mu^2\right) \tag{2}$$

Figure 2 shows $\bar{q} = fn(\mu)$ for a constant chord blade for the three conversion schedules. As seen here, a point of minimum rotor lifting capability is reached for each schedule, and μ_{crit} and $\bar{q}_{min}$ are dependent upon the method of conversion. For schedules A and B where V_∞ is constant, the critical advance ratio is 1.2, while the accelerating conversion (schedule C) has $\mu_{crit} = 1.0$.

In Figure 3, the same information is plotted as $\bar{q}/\rho V_T^2 = fn(\mu)$. The quantity $\bar{q}/\rho V_T^2$ can be related directly to the rotor thrust coefficient, C_T, by

$$C_T = \frac{\bar{C}_\ell \bar{c}}{\pi R} \cdot \left(\frac{\bar{q}}{\rho V_T^2}\right) \tag{3}$$

where $\bar{C}_\ell = L_{rotor}/(\rho/2\ \bar{V}_\ell^2\ \bar{c}\ R)$. Here, C_T is independent of the conversion schedule, and minimum C_T is reached at $\mu = 0.85$. Note that the thrust coefficient is not as directly relevant to a stoppable rotor (variable V_T) as it is to a conventional rotor. This is because the minimum C_T condition does not necessarily coincide with the minimum thrust condition for variable V_T rotors.

In Figure 4, $\bar{q}$ is plotted for constant V_∞ conversions beginning at various advance ratios. The dotted line shows $\bar{q}$ when dynamic pressure in the reverse flow region is not included, such as for a conventional rotor which cannot generate significant lift in reverse flow. This relative loss of $\bar{q}$ is much more directly proportional to the lift loss for these rotors than for CC rotors.

Beginning conversion at $\mu = 1.0$ ($V_\infty = V_T$) results in two critical advance ratios with equal $\bar{q}_{min}$. This also proves to be the condition under which the $\bar{q}$ at the end of conversion, $\bar{q}_{fw}$, is equal to the $\bar{q}$ in hover. Because

$$\bar{q}_{hover} = \frac{\rho}{\pi R^2} \int_{\pi}^{2\pi} \int_{0}^{R} \left(\frac{r}{R} V_T\right)^2 \ r\,dr\,d\psi \tag{4}$$

$$= \frac{\rho}{4} V_T^2$$

and

$$\bar{q}_{fw} = \frac{\rho}{\pi R^2} \int_{\pi}^{2\pi} \int_{0}^{R} (V_{fw} \sin \psi)^2 \, r dr d\psi \tag{5}$$

$$= \frac{\rho}{4} V_T^2 \mu_i^2$$

then

$$\bar{q}_{fw}/\bar{q}_{hover} = \mu_i^2 \tag{6}$$

where μ_i is the advance ratio at which conversion is initiated. Equation (6) is important to the designer because $\bar{q}_{fw}$ must be sufficient to permit steady, level flight in the fixed-wing mode immediately following conversion. Figure 5a shows a three-dimensional view of $\bar{q}$ for a matrix of possible flight conditions as were seen in Figure 1. Cutaway views (Figures 5b through 5d), corresponding to the conversions of Figure 4, provide another perspective of the effect of higher conversion speeds to increase $\bar{q}$ at the end of conversion and to provide higher $\bar{q}_{min}$ at the critical advance ratio.

The analysis can be applied to the effect of changing the rotor planform via taper ratio by using Equation (1) with the relation

$$c = \frac{2\bar{c}}{1+\lambda} \left[1 - (1-\lambda)\, x\right] \tag{7}$$

where λ = taper ratio = c_{tip}/c_{root}

$\bar{c}$ = mean chord

x = nondimensional span position = r/R

In this way, the effect of taper ratio and changes in blade area may be investigated independently.

The expression indicative of rotor lifting capability then becomes

$$\overline{qc} = \frac{2\rho\bar{c}}{\pi(1+\lambda)} V_T^2 \left\{\pi\left[\frac{1}{4} - \frac{(1-\lambda)}{5}\right] - 4\mu\left[\frac{1}{3} - \frac{(1-\lambda)}{4}\right] + \frac{\pi\mu^2}{4}\left[\frac{1}{2} - \frac{(1-\lambda)}{2}\right]\right\} \tag{8}$$

Figure 6 shows $\overline{qc} = fn(\mu,\lambda)$ for $0<=\lambda<=1$ for a typical conversion schedule. Tapering the blades reduces the magnitude of $\overline{qc}$ and also shifts μ_{crit} to lower values. However, the tapered blade experiences less loss of $\overline{qc}$ between μ_{crit} and the point at which conversion is initiated.

In addition to the magnitude of $\overline{qc}$, the lateral location

$$\epsilon_{RS} = \frac{\int_{\pi}^{2\pi}\int_{0}^{R} q(r,\psi) r \, crdrd\psi}{\int_{\pi}^{2\pi}\int_{0}^{R} q(r,\psi) \, crdrd\psi}$$

of the centroid of qc on the retreating side affects the roll moment created by $\overline{qc}$. An outboard centroid is desirable because it allows increased lift on the advancing side. Figure 7 shows the trend of this centroid to move inboard, then outboard as the rotor rpm is reduced. In fact, the most inboard position of the centroid occurs at advance ratios that coincide with the critical flight conditions discussed previously. Because lift on the advancing side of the rotor must balance the moment produced by the retreating side, lift must be reduced on the advancing side as ϵ_{RS} decreases. The combined effects of reduced $\overline{qc}$ and inboard travel of the qc centroid amplify the critical nature of this flight region as the capability of the rotor to produce lift in a trimmed state is further degraded.

To verify the presence of μ_{crit} and the ability of this analysis to predict its location, $\overline{qc}$ and $\overline{qc\epsilon}$ trends are compared in Figure 8 with rotor lift predictions (trimmed in roll moment) from a rigorous blade element strip integration analysis described by Rogers.[1] Note that "percent relative lift" is much greater than "percent relative $\overline{qc}$" at μ_{crit}. This, again, is because CC rotor lift is not directly proportional to the dynamic pressure. The simple analysis predicts μ_{crit} to be in the range of 0.9 to 1.2, which is slightly higher than the more rigorous method. Differences can be attributed to inflow effects and the lifting capability of the rotor's advancing side.

REMARKS

Simple algebraic expressions have been derived which provide an indicator of the relative lifting capability of a stoppable rotor and can qualitatively identify the critical flight condition of a rotor in terms of lifting capability. First-order effects of rotor planform geometry (taper ratio, root cutout, and blade span) and operational conditions (conversion speed and tip speed) on conversion performance can be readily obtained using the techniques described. Additional, sophisticated analytical methods are necessary to provide more precise quantitative information.

REFERENCE

1. Rogers, E.O., "Recent Progress in Performance Prediction of High Advance Ratio Circulation Controlled Rotors," Tech Paper No. 29 presented at Sixth European Rotorcraft and Powered Lift Aircraft Forum, Bristol, England (16-19 Sep 1980).

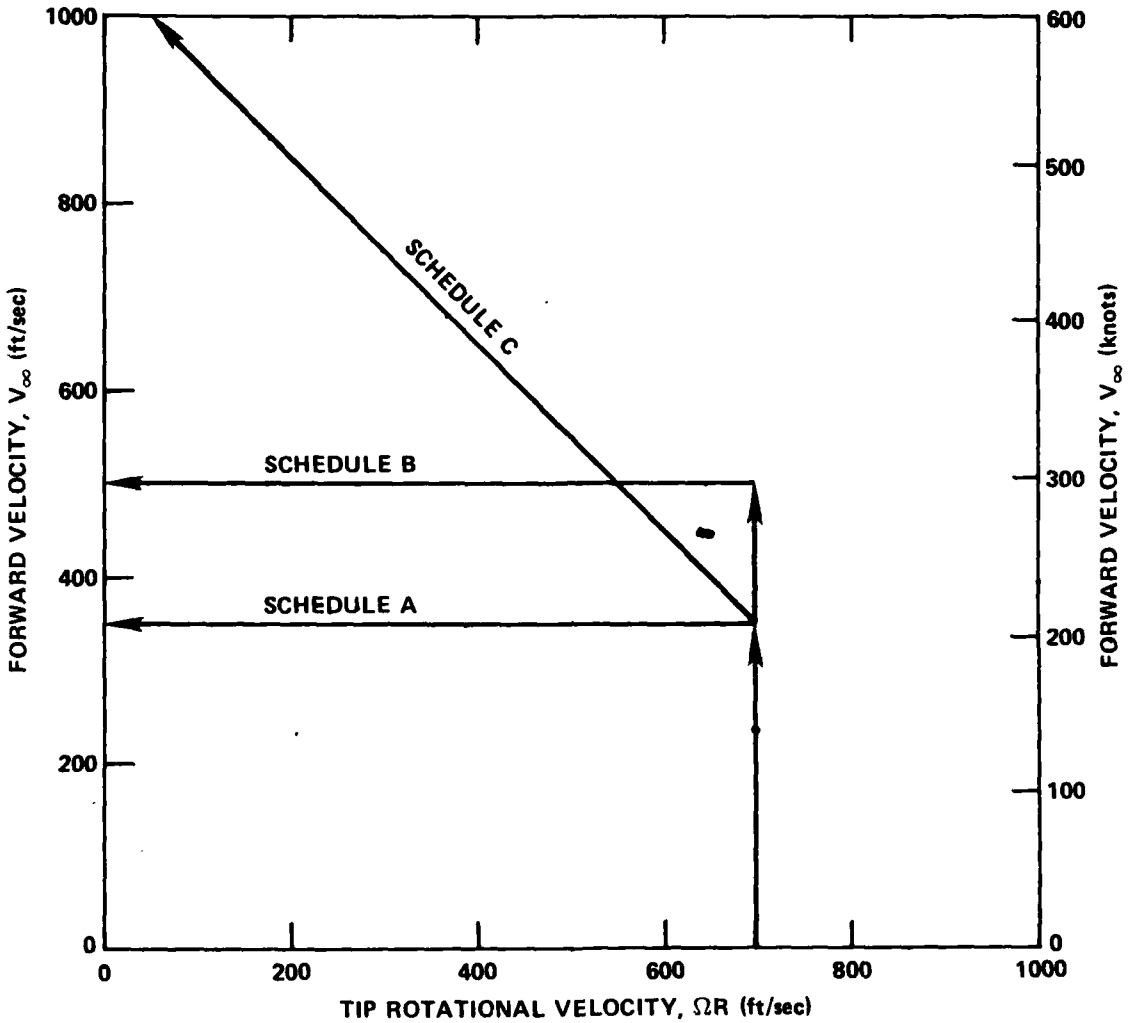

Figure 1 - Typical X-Wing Rotor Conversion Schedules

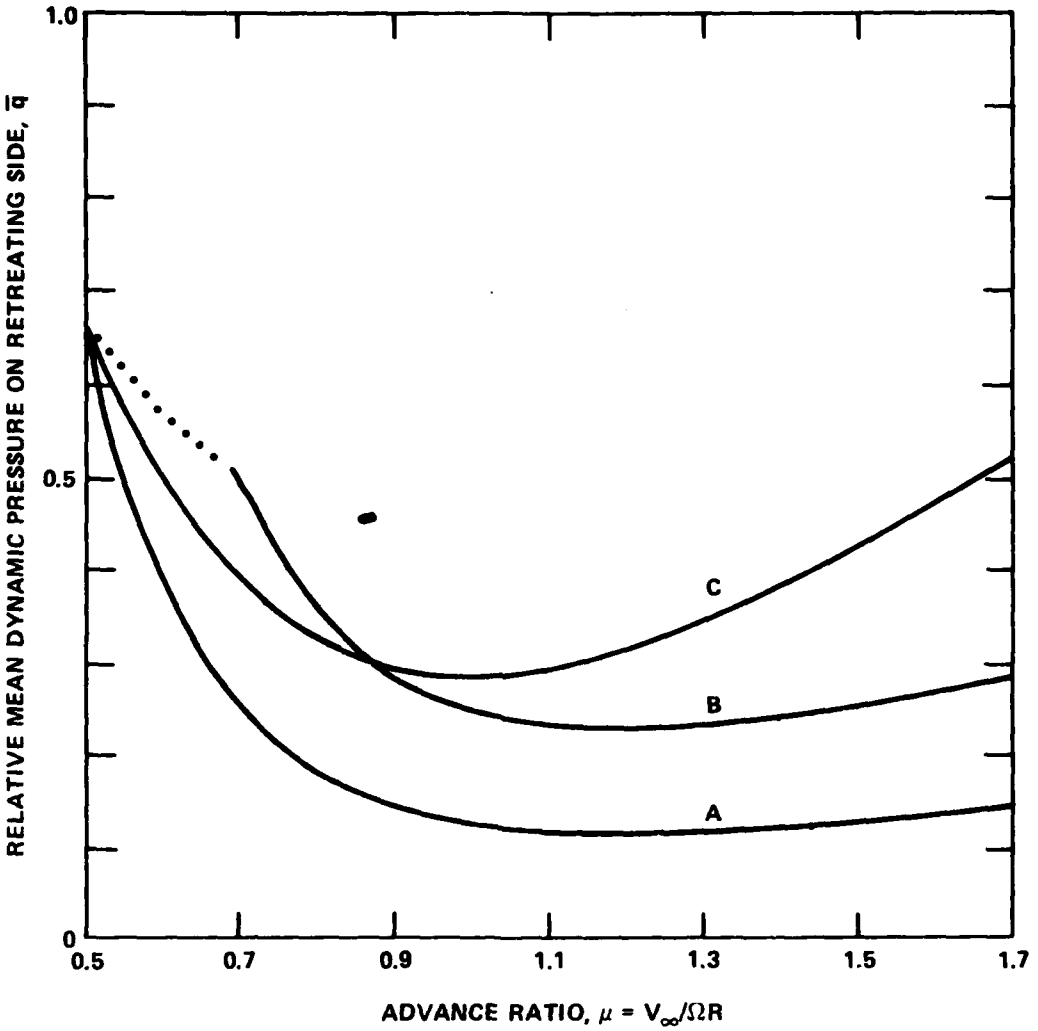

Figure 2 - Identification of Critical Conditions for Conversion Schedules A, B, and C

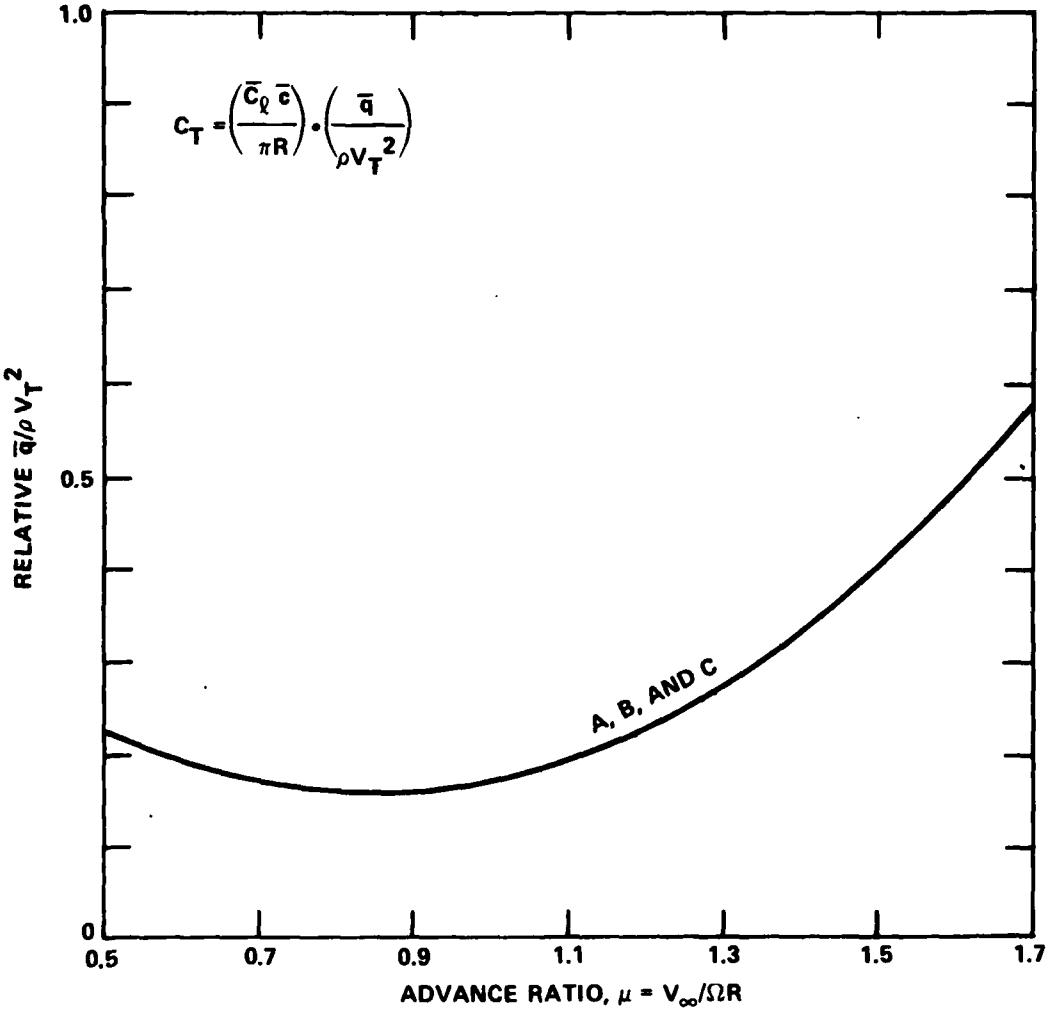

Figure 3 - Characteristics of Rotor Thrust Coefficient Capability

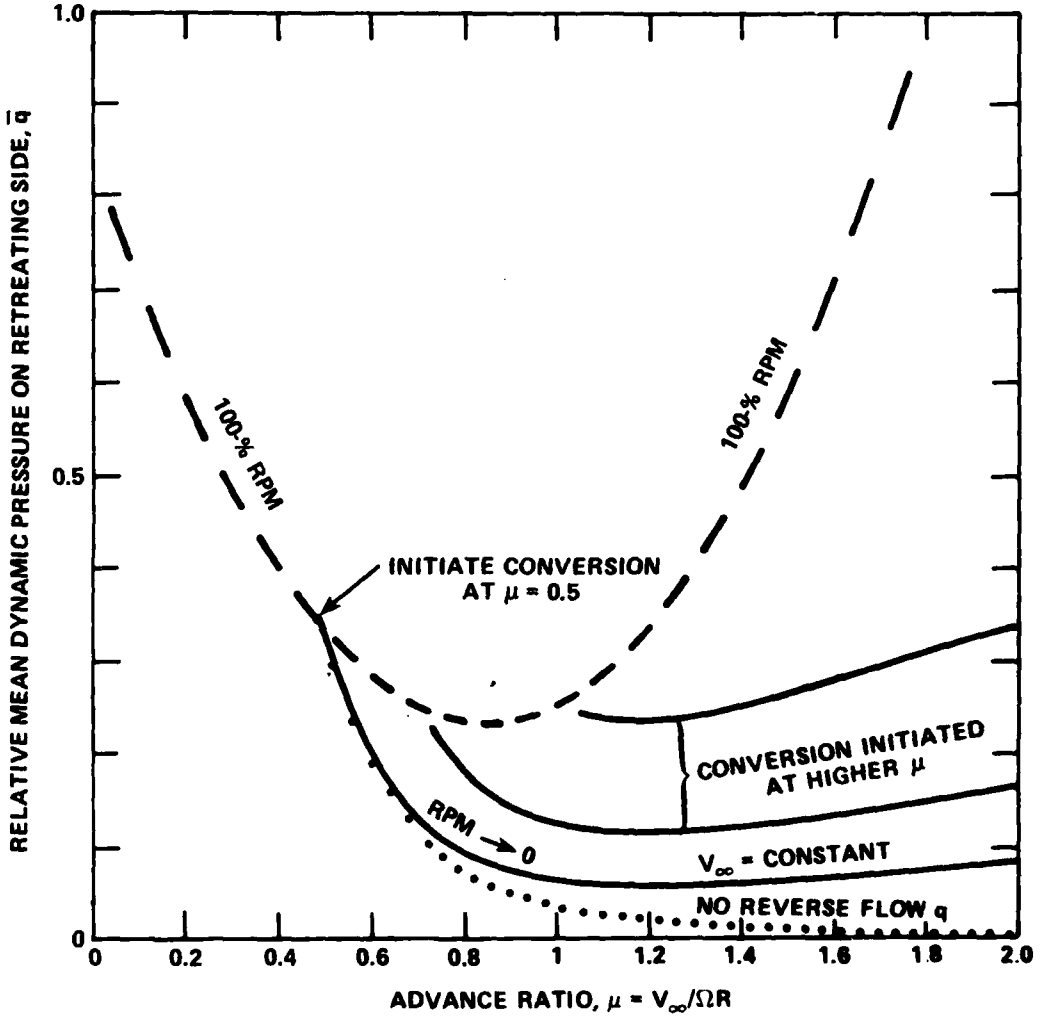

Figure 4 - Characteristics of Rotor Lifting Capability

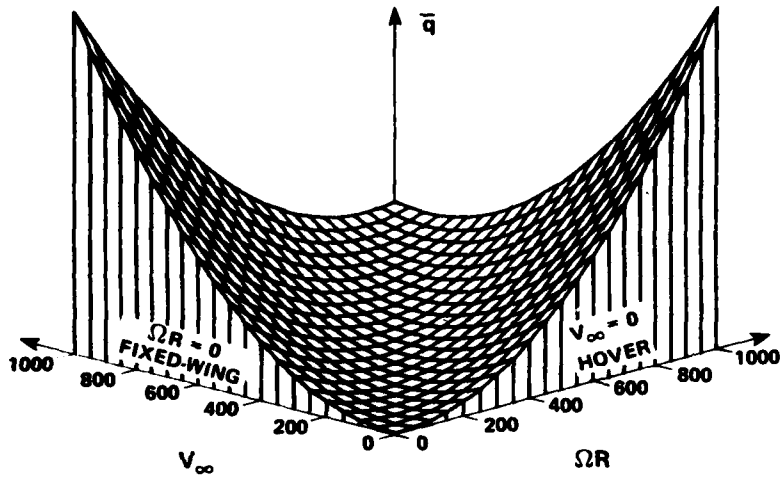

Figure 5a

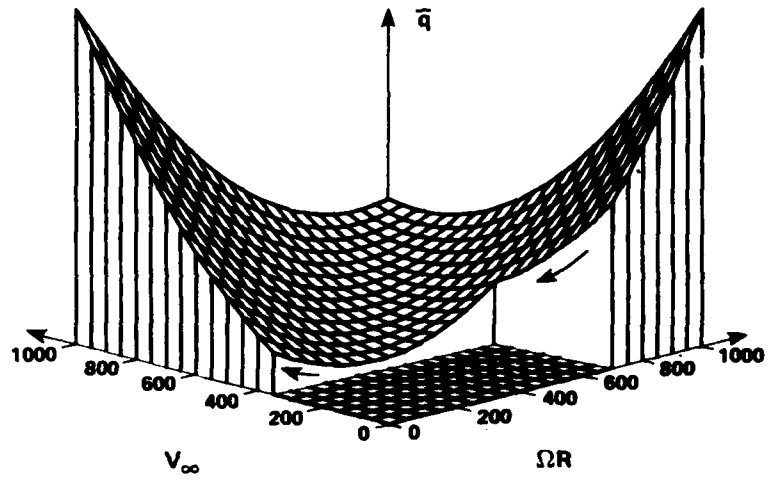

Figure 5b - $\mu_i = 0.5$

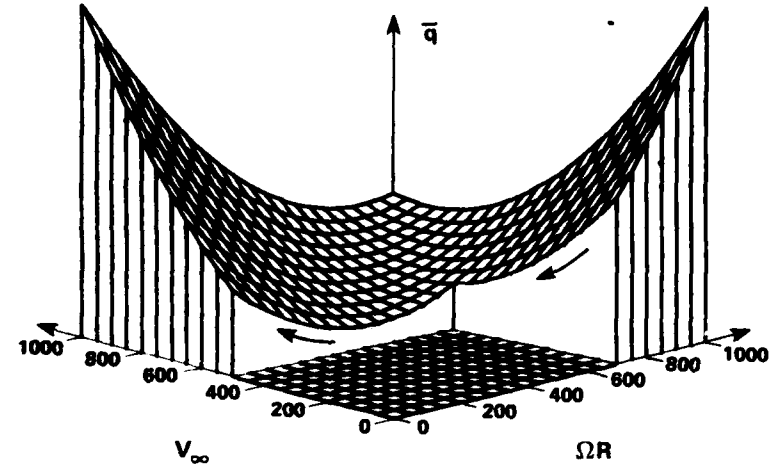

Figure 5c - $\mu_i = 0.7$

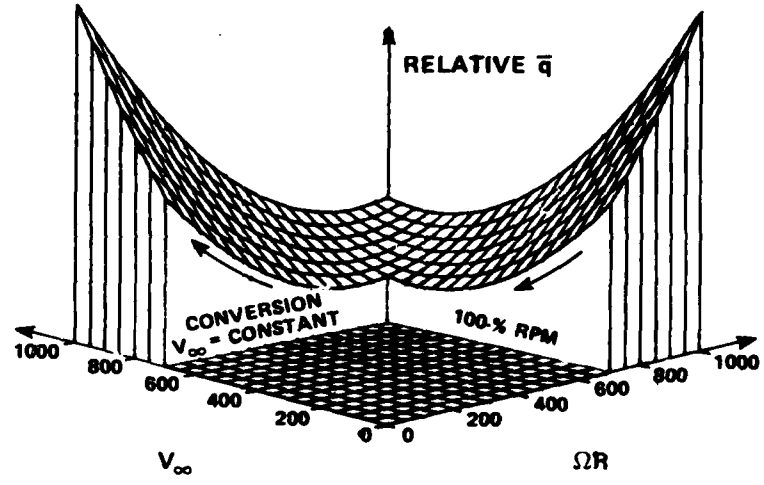

Figure 5d - $\mu_i = 1.0$

Figure 5 - Effect of Conversion Speed on Rotor Mean Dynamic Pressure
(Conversions from Figure 4)

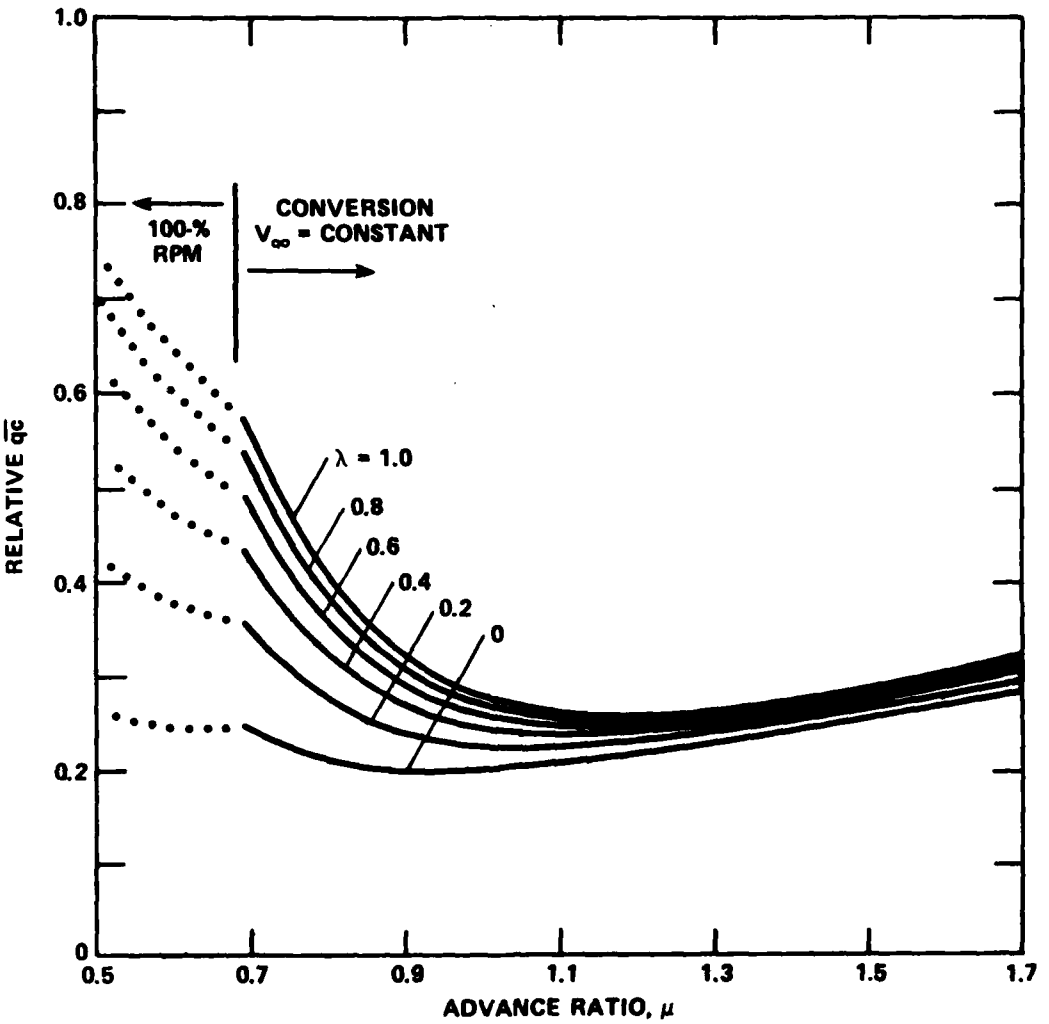

Figure 6 - Effect of Blade Planform on Critical Condition

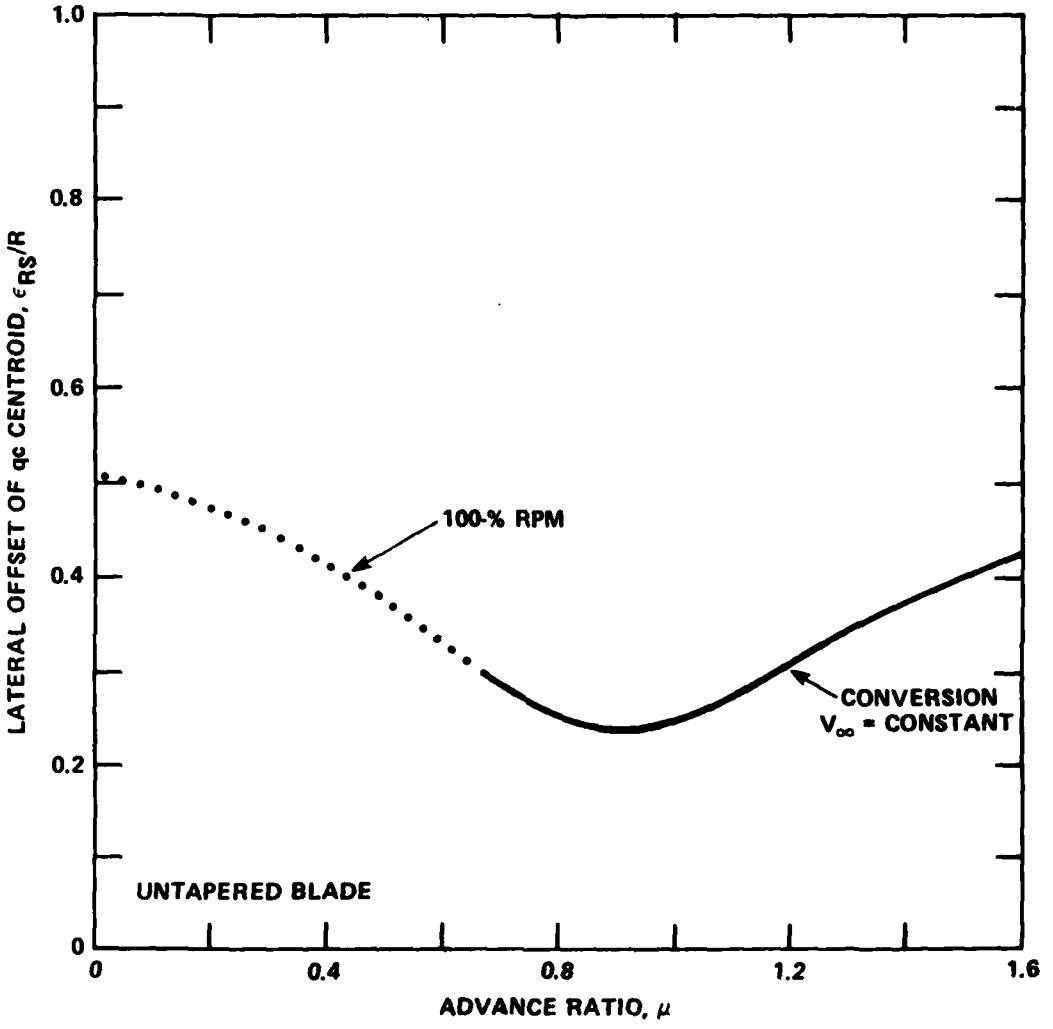

Figure 7 - Characteristics of Retreating Side Roll Moment Arm

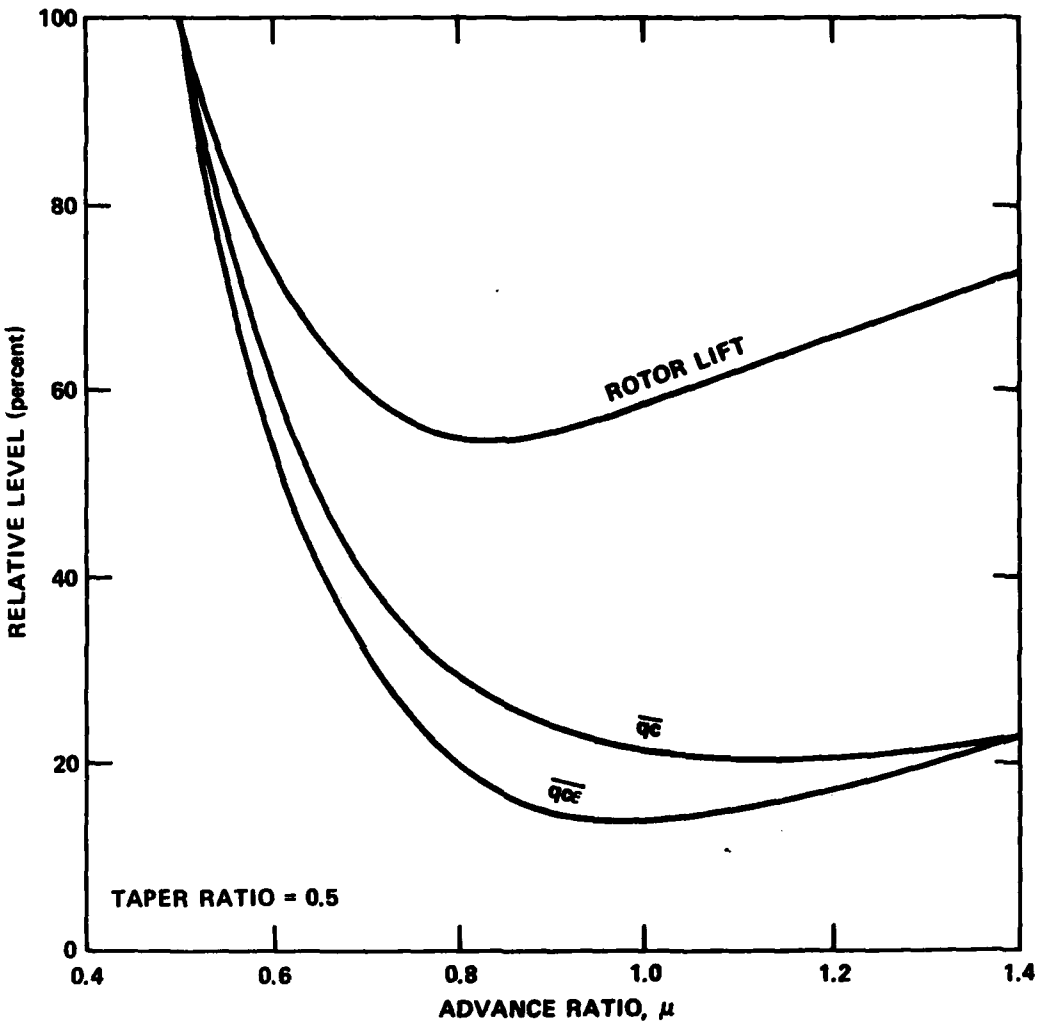

Figure 8 - Comparison of Mean Dynamic Pressure Trends with Sophisticated Rotor Performance Analysis

DTNSRDC ISSUES THREE TYPES OF REPORTS

1. DTNSRDC REPORTS, A FORMAL SERIES, CONTAIN INFORMATION OF PERMANENT TECHNICAL VALUE. THEY CARRY A CONSECUTIVE NUMERICAL IDENTIFICATION REGARDLESS OF THEIR CLASSIFICATION OR THE ORIGINATING DEPARTMENT.

2. DEPARTMENTAL REPORTS, A SEMIFORMAL SERIES, CONTAIN INFORMATION OF A PRELIMINARY, TEMPORARY, OR PROPRIETARY NATURE OR OF LIMITED INTEREST OR SIGNIFICANCE. THEY CARRY A DEPARTMENTAL ALPHANUMERICAL IDENTIFICATION.

3. TECHNICAL MEMORANDA, AN INFORMAL SERIES, CONTAIN TECHNICAL DOCUMENTATION OF LIMITED USE AND INTEREST. THEY ARE PRIMARILY WORKING PAPERS INTENDED FOR INTERNAL USE. THEY CARRY AN IDENTIFYING NUMBER WHICH INDICATES THEIR TYPE AND THE NUMERICAL CODE OF THE ORIGINATING DEPARTMENT. ANY DISTRIBUTION OUTSIDE DTNSRDC MUST BE APPROVED BY THE HEAD OF THE ORIGINATING DEPARTMENT ON A CASE-BY-CASE BASIS.